Differential roles of extracellular matrix proteins on primary and metastatic pancreatic cancer cells

Olalekan Usman[1], Sampath Kumar[1], Reddick R Walker III[1], Gengqiang Xie[1], AbdelAziz R. Jalil[3], Subramanian Ramakrishnan[2], Lawrence J. Dooling[3], Yue Julia Wang[1], Jerome Irianto[1]*

1. Department of Biomedical Sciences, College of Medicine, Florida State University, Tallahassee, FL, 32306, USA
2. Department of Chemical and Biomedical Engineering, FAMU-FSU College of Engineering, Tallahassee, FL, 32310, USA
3. Physical Sciences Oncology Center at Penn, University of Pennsylvania, Philadelphia, PA, USA

*Corresponding author: Jerome Irianto, Department of Biomedical Sciences, College of Medicine, Florida State University, 1115 West Call St, Tallahassee, FL 32306.
Phone: 850-645-9438
E-mail: jerome.irianto@med.fsu.edu

Abstract

Pancreatic cancer adenocarcinoma (PDAC) has been reported to be the third highest cause of cancer-related deaths in the United States. PDAC is known for its high proportion of stroma which accounts for 90% of the tumor mass. The stroma is made up of extracellular matrix (ECM) and non-malignant cells such as inflammatory cells, cancer-associated fibroblasts (CAF), and lymphatic and blood vessels. Here, we decoupled the roles of the extracellular matrix on PDAC cell lines by investigating the effects of different ECM proteins on the cell lines. Our data showed that primary lines have different morphology that depends on the ECM proteins on which they are cultured, while metastatic PDAC lines' morphology does not change with respect to different ECM proteins. Next, we examined how these ECM proteins affect the cell response to the gemcitabine's cytotoxicity. Lastly, transcriptomics analysis of the cells cultured on different ECM reveals the regulation of various pathways, such as cell cycle, cell adhesion molecules, and focal adhesion, including the regulation of several integrin genes that are essential for ECM recognition.

Introduction

Pancreatic cancer adenocarcinoma (PDAC) has been reported to be the third highest cause of cancer-related deaths in the United States and it is predicted to be ranked second before 2030, replacing colorectal cancer [1,2]. Although, in general, there has been a downward trend in the number of cancer deaths with a 32 percent decrease from its peak in 1991 and 2019 [3], PDAC has been an exception, with less than 5% of the patients surviving for 5 years [4]. This poor prognosis has been attributed to the difficulty in early-stage diagnosis due to the lack of specific tumor markers, resistance to radiotherapy, chemotherapy, and molecular targeted therapy [5]. PDAC is known for its high proportion of stroma which accounts for 90% of the tumor mass [6]. The stroma is made up of extracellular matrix (ECM) and non-malignant cells such as inflammatory cells, cancer-associated fibroblasts (CAF), and lymphatic and blood vessels. These stromal components are in a bidirectional dynamic interaction with the tumor cells [7]. Tumor fibrotic stroma has been a major contributor to PDAC progression, and invasion, together with resistance to treatment [8], [9]. The resulting stiffness from high stroma deposition in PDAC can also result in deformation of the vasculature, thereby limiting oxygen, nutrients, and drug transport to the tumor cells [10].

Extracellular matrix is a highly organized 3-dimensional meshwork that surrounds and provides physical support for the cells [11]. ECM is mainly made up of glycoproteins and fibrous proteins that include collagens, fibronectin, laminin, vitronectin, proteoglycans, and elastin [12],[13]. The reorganization, density, posttranslational modifications, and remodeling of its constituent proteins confer the ECM the ability to respond to both biochemical and mechanical cues from the tumor microenvironment [14]. Fibrillar fibronectin is required for collagen fibers to assemble. Of the 28 collagens that have been identified, collagen I is known to promote tumorigenesis, and immunohistochemistry staining from different studies showed a significantly high level of the protein in both mouse and human PDAC samples [15], [16]. Laminin is involved in providing tensile strength in the basement membrane which helps to maintain the apical-basal polarity of epithelial structures.

Here, we decoupled the roles of the extracellular matrix on PDAC cell lines by investigating the effects of different ECM proteins on the lines. Our data showed that primary lines have different morphology that depends on the ECM proteins on which they are cultured while metastatic PDAC lines morphology does not change with respect to different ECM proteins. Next, we examined how these ECM proteins affect the cell response to the gemcitabine's cytotoxicity. Lastly,

transcriptomics analysis showed differential expression of genes involved in pathways such as MAPK signaling pathway, cell cycle, DNA replication, etc., when MIA Paca-2 was cultured on different ECM proteins. Finally, we observed differences in integrins levels for cells cultured in vitronectin and fibronectin which might explain the difference in unique pathways regulated in the two ECM proteins.

Results

Extracellular matrix proteins have different effects on pancreatic ductal adenocarcinoma (PDAC) cell lines morphology and proliferation

To study the effect of extracellular matrix proteins on the morphology of the cell, primary pancreatic ductal adenocarcinoma cell lines (MIA Paca-2 and Panc-1) were seeded at approximately 3200 cells/cm^2 and cultured for 6 days in well plates coated with laminin, collagen I, fibronectin and vitronectin. Microscopy imaging shows that MIA Paca-2 spreads in wells coated with fibronectin and vitronectin, similar to cells grown with fetal bovine serum while they are rounded in laminin and collagen in a manner similar to cells grown on a plate with no ECM protein coating (**Figure 1A top**). The Panc-1 line adheres and spreads on fibronectin, vitronectin, and collagen I substrates while they were rounded on laminin (**Figure 1A Bottom)**. We quantified the morphology of the cells grown on each substrate by estimating the aspect ratio of 30 cells randomly selected from 20X images using ImageJ. Our quantification shows that MIA Paca-2 and Panc-1 on vitronectin and fibronectin substrates have a significantly higher aspect ratio compared to cells cultured on plates without any protein coating and laminin (**Figure 1A, plots)**. AsPC-1 and Capan-1, which are derived from metastatic sites of a pancreatic ductal adenocarcinoma patient [17], were also cultured on plates coated with different ECM proteins. Microscopy imaging reveals that these cell lines moderately spread in all the substrates and wells with no ECM coating. Estimation of the aspect ratio showed that the morphology of the cell lines does not change with respect to different substrates **(Figure 1B)**. Capan-1 cells are often clustered together and to quantify their aspect ratio, we stained the with DAPI and phalloidin which allows us to differentiate between membranes of cells in a cluster.

Additionally, we studied the effect of the substrates on the growth of the cell lines using a luminescence assay. MIA Paca-2, PANC-1, AsPC1, and Capan-1 cell lines were cultured on surfaces coated with collagen I, fibronectin, laminin, and vitronectin. The number of cells under each condition was quantified on days 2, 4, and 6 using a luminescent cell viability assay. The number of cells on days 2, 4, and 6 was normalized to the number of cells seeded. This reveals

that MIA Paca-2 on vitronectin, and fibronectin substrates have a significantly higher proliferation rate when compared to those cells on laminin and collagen I **(Figure 1Ci)**. Panc-1 cultured on fibronectin, collagen I, and vitronectin substates double faster relative to those cultured on laminin **(Figure 1Cii)**. Also, we found out that AsPC-1 and Capan-1 proliferation rate is not significantly influenced by any of the ECM proteins we grew them on **(Figure 1Ciii-iv)**.

Extracellular matrix proteins alter cell response to gemcitabine

Gemcitabine is an analog of deoxycytidine [18], used as the first-line treatment for PDAC patients [19]. However, after a few weeks of treatment, most patients become resistant to the drug [20]. To assess the cytotoxic effect of gemcitabine on the cell lines, we treated them with gemcitabine for 72 hours and the cell numbers were estimated using a luminescence cell viability assay. We found that MIA Paca-2 and Capan-1 are more sensitive to the drug treatment, with IC50 of 10.8 and 2.8 nM, compared to Panc-1 and AsPC-1 with IC50 of 544.2 and 652.9 nM, respectively **(Figure 2B).**

PDAC is known for its high stroma which has been implicated in chemoresistance [21]. Next, we tested the effect of specific ECM proteins on the response of MIA Paca-2 and Capan-1 after treatment with gemcitabine. Towards this, we cultured MIA Paca-2 on surfaces coated with different ECM proteins and then treated with gemcitabine to study how the ECM proteins affect drug response. The cell viability plot shows that the total number of surviving cells after gemcitabine treatment is the lowest for cells cultured in FBS, followed by the cells cultured on fibronectin and vitronectin (ECM proteins in which the cell has a spread morphology) compared to no ECM, **(Figure 2C)**. In contrast, ECM proteins do not significantly alter the decrease in the number of surviving cells following drug treatment in Capan-1 cells cultured on different substrates **(Figure 2D)**.

ECM proteins result in differential gene expression

To investigate the roles of different ECM proteins on gene expression in MIA Paca-2, RNA was extracted from cells cultured on surfaces without (no ECM) or with ECM protein coating: collagen I, laminin, fibronectin, and vitronectin (media supplemented with 2% B27), and on media supplemented with 10% FBS. MIA Paca-2 cell line was used for this experiment because it is one of the lines that showed difference in growth and morphology with respect to different ECM proteins. Next, we performed RNA-seq and analyzed the transcriptome. The gene count across the conditions was normalized using the variance stabilizing transformation from DESeq2 [22]. The sample clustering was visualized by plotting the first two components resulting from PCA analysis

on the x and y axes respectively. PCA analysis showed that cells on ECM proteins (collagen I, laminin) that result in rounded morphology clustered together with cells grown on no ECM. Interestingly, cells cultured on ECM proteins that result in spread morphology (fibronectin and vitronectin) cluster separately from each other, and the cells cultured in FBS. Taken together, this result corresponds with the morphology and proliferation rate results shown in **Figure 1A-C**. Also, it suggests that ECM protein on which the cell was cultured affects the gene expression **(Figure 3A).** Furthermore, we showed the difference in the gene expression pattern in cells cultured on different substrates by making a heatmap with normally read counts of the differentially expressed genes using the pheamap package in R [23]. To make this heatmap, significant differentially expressed genes (adjusted p-value < 0.05, abs($\log_2$FC) > 0.58) in all the ECM proteins were combined and clustered by K-mean (with centers = 4) resulting in the color-coded clusters. Hierarchical clustering was used to cluster the column using Pearson's correlation and Ward.D2. Clustering analysis of the heatmap reveals that cells cultured on collagen I, laminin, and no ECM protein have a similar expression pattern while those cultured on fibronectin, vitronectin, and FBS show differential gene expression patterns **(Figure 3B)**. Cluster 1 comprises genes that are highly upregulated in cells cultured in FBS, while also generally upregulated in cells cultured on vitronectin and fibronectin. Cluster 2 comprises genes that are downregulated in cells cultured in 10% FBS. Clusters 3 and 4 comprise genes that are upregulated and downregulated in cells cultured on a surface coated with vitronectin, respectively **(Figure 3B)**. With the aim of investigating the pathways up(down)regulated in each cluster, we did the functional annotation analysis with Enrichr using genes in each cluster [24]. Cluster 1 contains genes that are upregulated in FBS and are enriched for cell cycle, DNA replication, RNA transport, spliceosome, and other pathways **(Figure 3Ci)**. Cluster 2 consists of genes that are uniquely downregulated in FBS and are enriched in pathways involving lysosome and glycosaminoglycan **(Figure 3Cii)**. Cluster 3 is made up of genes that are uniquely upregulated in vitronectin and enriched in pathways that include MAPK signaling, cell adhesion molecules, axon guidance, wnt signaling pathway, and so on **(Figure 3Ciil)**. Cluster 4 contains genes that are uniquely downregulated in vitronectin and are enriched in pathways such as terpenoid backbone biosynthesis, endocytosis, and focal adhesion.

Having found that culturing MIA Paca-2 cell lines on different extracellular matrix protein results in a differential gene expression, we tried to uncover the pathways that are upregulated and downregulated in both fibronectin and vitronectin, and the ones unique to either vitronectin or fibronectin only. To achieve this, we filtered genes that are differentlially expressed, significant, and have a fold change higher than 1.5X in both fibronectin and vitronectin. We found that 167

genes were upregulated in MIA Paca-2 cultured in both fibronectin and vitronectin, while 868 and 126 genes are upregulated in vitronectin and fibronectin respectively (**Figure 4A left**). 335 genes were downregulated in both fibronectin and vitronectin while 1265 and 297 genes were downregulated in vitronectin and fibronectin respectively (**Figure 4A right)**. To elucidate the pathways that are enriched for genes that are differentially regulated in fibronectin and vitronectin (the overlap of the Venn diagram in **Figure 4A**), and only in fibronectin or vitronectin, were subjected to pathway analysis using the Enrichr and a maximum of top 10 significant KEGG pathways were selected (FDR < 0.1). The analysis revealed that pathways involved in tight junction, regulation of actin cytoskeleton, and proteoglycans in cancer are upregulated in fibronectin and vitronectin while pathways involved in Parkinson's disease, oxidative phosphorylation, diabetic cardiomyopathy, prion disease, etc (**Figure 4B)**. Pathways involved in focal adhesion are upregulated in vitronectin only while those involved in Wnt signaling, axon guidance, hippo signaling, etc are downregulated (**Figure 4C)**. Also, cell cycle, oocyte meiosis, and cellular senescence pathways are upregulated in fibronectin only while mineral absorption is downregulated (**Figure 4D)**. Further look into the transcriptomic data, we observed differential expression of several integrin genes in MIA Paca-2 cells cultured on vitronectin and fibronectin (**Figure 4E)**. Both *ITGB8* and *ITGA6* were downregulated in cells cultured on fibronectin and vitronectin. *ITGA10* was uniquely downregulated in the fibronectin group, while *ITGB4* and *ITGB6* were uniquely upregulated in cells cultured on the vitronectin surface.

Discussion

High desmoplastic stroma of the PDAC has been reported to contribute to tumor progression, stiffness, invasion, and chemoresistance by hindering the delivery of drugs [27,28]. Compared to normal tissues, higher levels of ECM proteins such as collagen I, fibronectin, and so on, are detected in the tumor stroma, and their levels correspond with cancer progression [29-31]. In this study, we investigated the morphology, proliferation, and response to the gemcitabine of PDAC cells in the presence of collagen I, fibronectin, laminin, and vitronectin. In addition, we used transcriptomics and gene ontology analysis to identify pathways differentially regulated in different ECM proteins.

When we cultured MIA Paca-2, Capan-2, and AsPC-1 on plates coated with collagen I, fibronectin, laminin, and vitronectin. We observed that MIA Paca-2 cells are rounded in laminin and collagen I while they spread in vitronectin and fibronectin. Panc-1 cells are rounded in laminin but they adhere and spread in collagen I, fibronectin, and collagen (**Figure 1A**). Our result

validates previous reports [32]. Also, in accordance with published results [33], we observed that fibronectin and vitronectin increase the proliferation of MIA Paca-2. Collagen I, fibronectin, and vitronectin increase the proliferation of Panc-1 (**Figure 1B**). The metastatic cell lines (AsPc-1 and Capan-1) adhere and spread in the ECM just as in the uncoated well plate, but they do not show a significant increment in proliferation, suggesting that the PDAC lines' response to ECM proteins is cell line dependent. Gemcitabine is a widely used drug to treat PDAC but over time the cancer cells become resistant to it [34]. We found that the cells' sensitivity to gemcitabine increases when they spread and adhere to the ECM substrate (**Figure 2**). This suggests a relationship between drug uptake and cell adhesion. Gene ontology showed unique upregulations of genes that are involved in cell adhesion and cell cycle in MIA Paca-2 that was cultured on vitronectin (**Figure 3C**). In addition, genes upregulated in MIA Paca-2 fibronectin and vitronectin partake in pathways (such as tight junction, regulation of actin cytoskeleton) that have been reported to be involved in cell adhesion (**Figure 4B**) [35]. Although MIA Paca-2 cells spread both on vitronectin and fibronectin, we observed differences in pathways regulated by both substrates. Considering the critical role of integrin in focal adhesion and ECM recognition, this might be a result of the differential expression of integrin molecules that connect the cells to the substrate (**Figure 4E**). It is noteworthy to mention that our study is limited to 2D culture. Indeed, we did not observe differences in MIA Paca-2 spheroid growth within the 3D polyethylene glycol (PEG) culture containing different ECM proteins (**Figure S1 A-B).** Even though the patient-derived pancreatic cancer organoid grows in our PEG hydrogel and patient-derived glioblastoma organoids invade to their surroundings in the presence of laminin (**Figure S1 C-F)**. Nevertheless, in this study, we have shown that ECM proteins affect the morphology, proliferation, and response to drug treatment of PDAC cells. Furthermore, we identified pathways uniquely regulated by some of the ECM proteins, including some of the integrins.

Experimental procedures

Cell culture

MIA Paca-2 and PANC-1, pancreatic ductal adenocarcinoma (PDAC) primary cell lines, were cultured in DMEM high-glucose media (Genesee Scientific). The PDAC metastatic cell lines used, AsPC-1 and Capan-1, were cultured in RPMI 1640 media (Genesee Scientific). Both media were supplemented with 10% fetal bovine serum (FBS) (Sigma-Aldrich) and 1% penicillin and streptomycin (Corning). For experiments to study the effects of ECMs, 2% B-27 Supplement (ThermoFisher) was used in place of FBS. Both the PDAC and glioblastoma organoids were acquired from ATCC, as part of the Human Cancer Models Initiative with the organoid name HCM-

CSHL-0092-C25 (ATCC PDM-39) and HCM-BROD-0103-C71 (ATCC PDM-121), respectively. Maintenance of the organoid culture was performed following the instructions from ATCC.

Cell proliferation assay

Cells were seeded at 3200-6400 cells/cm2 and cultured for 6-9 days, and their number was measured every 2-3 days using the CellTitre-Glo 3D cell viability assay (Promega), as described by the manufacturer. Briefly, cells were seeded in a white-bottom 96-well plate coated with different ECM proteins for 2, 4, 6, and 9 days respectively. The CellTitre-Glo reagent is added to the wells (1:1). The plate reader (BioTek Synergy H1MF multi-mode) shakes the plate for 2 minutes with a delay time of 10 minutes after which the luminescence is measured and recorded. The number of cells is extrapolated from the standard curve generated for the luminescence readings.

Immunofluorescence and image processing

Cells/hydrogels were fixed in 4% formaldehyde (Electron Microscopy Sciences) after which they were permeabilized in 0.25% Triton X-100 (MilliporeSigma) for 10 minutes and blocked with 5% bovine serum albumin (VWR Chemicals) for 30 mins and incubated overnight with primary antibodies. They were incubated in secondary antibodies for 1.5 hours. For nuclei and F-actin staining, cells were incubated in 2μg/ml DAPI and phalloidin-tetramethyrhodamine B isothiocyanate (Sigma-Aldrich) respectively, for 1 hour. Images were taken with an Olympus microscope 20x/0.75 NA or 40x/0.6 NA objective. All the image analysis was done with Image [36].

3D PEG hydrogel culture

3D PEG gel precursors (PEG-NDG-Lys, (PEG-Gln) were made as described in [37]. Briefly, NDG-Lys and Gln peptides (GenScript) were dissolved in triethanolamine (0.3 M, pH 8.0) and incubated with PEG-VS (8 arms) (JemKem Technology) at 37°C for 20 minutes. The PEG-NDG-Lys and PEG-Gln were lyophilized at 4°C for 4 days and lyophilized for 3 days. The resulting powder precursors (PEG-NDG-Lys, PEG-Gln) were dissolved and reconstituted in deionized water to make 13.33% w/v stock solution (PEG-NDG-Lys + PEG-Gln). TBS (50 mM, pH 7.6), fibronectin (Sigma-Aldrich) or collagen I (Corning) or laminin (Corning) or vitronectin (Sigma-Aldrich), and cells were added to the PEG-NDG-Lys + PEG-Gln solution. After the addition of thrombin-activated FXIII (CSL Behring) that triggers hydrogel formation, the mixture is incubated at 37°C for 30 minutes.

ECM proteins coating

Fibronectin (Sigma-Aldrich), collagen I (Corning), laminin (Corning), and vitronectin (Sigma-Aldrich) were coated on a plate according to the manufacturers' description. In short, plates are incubated with fibronectin and laminin for 1hr at room temperature. The collagen is coated overnight at 4°C. The plates are incubated with vitronectin at 37°C for 2hrs after which it's transferred to 4°C overnight.

Transcriptomics sample preparation and analysis

RNA-Seq library was prepared using the NEBNext Ultra II Directional RNA Library Prep Kit for Illumina (NEB) following the manufacturer's instructions. The library was sequenced on the Novaseq 6000 at Florida State University Translational Science Laboratory. This gives ~20 million reads per sample. The quality of the fastq reads from the sequencing was ascertained with FastQC [38] after which they were aligned with the hg19 human reference genome using the STAR software [39]. Library sizes were scaled and normalized with median of ratios using the DESeq2 package. Differential expression was estimated using the result function in DESeq2. Adjusted p-values using the Benjamini–Hochberg method was computed, and this is used to filter for significant genes. Pathway way analysis was done using the Enrichr [24].

Gemcitabine treatment

Cells were plated in either an ECM coated or regular white-bottom 96 well plate and treated after 24 h with gemcitabine (MilliporeSigma). Concentrations were chosen to encompass the clinically approachable concentrations of the drug. After 72 h, 100 ul of CellTiterGlo (Promega) was added to each well and shaken for two minutes, followed by 10 minutes incubation. Luminescence was measured using a microplate reader. Gemcitabine sensitivity curves and IC_{50} values were calculated using GraphPad Prism 9 (GraphPad).

Acknowledgment

The authors in this study were supported by startup funds from Florida State University, an award from the Florida Department of Health's Bankhead-Coley Cancer Research Program (award number 21B11), and a collaborative Trans-Network Project linked to the Physical Science-Oncology Project 5U01 CA214282 from the National Cancer Institute of the National Institutes of Health. Corifact is a gift from CSL Behring. The pancreatic cancer and glioblastoma organoid line is from the Human Cancer Models Initiative, https://ocg.cancer.gov/programs/HCMI.

References

1 Rahib, L. et al. Projecting cancer incidence and deaths to 2030: the unexpected burden of thyroid, liver, and pancreas cancers in the United States. Cancer Res 74, 2913-2921, doi:10.1158/0008-5472.CAN-14-0155 (2014).

2 Siegel, R. L., Miller, K. D. & Jemal, A. Cancer statistics, 2019. CA Cancer J Clin 69, 7-34, doi:10.3322/caac.21551 (2019).

3 Islami, F. et al. Annual Report to the Nation on the Status of Cancer, Part 1: National Cancer Statistics. J Natl Cancer Inst, doi:10.1093/jnci/djab131 (2021).

4 Hidalgo, M. Pancreatic cancer. N Engl J Med 362, 1605-1617, doi:10.1056/NEJMra0901557 (2010).

5 Kleeff, J. et al. Pancreatic cancer. Nat Rev Dis Primers 2, 16022, doi:10.1038/nrdp.2016.22 (2016).

6 Neesse, A. et al. Stromal biology and therapy in pancreatic cancer. Gut 60, 861-868, doi:10.1136/gut.2010.226092 (2011).

7 Feig, C. et al. The pancreas cancer microenvironment. Clin Cancer Res 18, 4266-4276, doi:10.1158/1078-0432.CCR-11-3114 (2012).

8 Perez, V. M., Kearney, J. F. & Yeh, J. J. The PDAC Extracellular Matrix: A Review of the ECM Protein Composition, Tumor Cell Interaction, and Therapeutic Strategies. Front Oncol 11, 751311, doi:10.3389/fonc.2021.751311 (2021).

9 Bijlsma, M. F. & van Laarhoven, H. W. The conflicting roles of tumor stroma in pancreatic cancer and their contribution to the failure of clinical trials: a systematic review and critical appraisal. Cancer Metastasis Rev 34, 97-114, doi:10.1007/s10555-014-9541-1 (2015).

10 Stylianopoulos, T. et al. Coevolution of solid stress and interstitial fluid pressure in tumors during progression: implications for vascular collapse. Cancer Res 73, 3833-3841, doi:10.1158/0008-5472.CAN-12-4521 (2013).

11 Mouw, J. K., Ou, G. & Weaver, V. M. Extracellular matrix assembly: a multiscale deconstruction. Nat Rev Mol Cell Biol 15, 771-785, doi:10.1038/nrm3902 (2014).

12 Kai, F., Drain, A. P. & Weaver, V. M. The Extracellular Matrix Modulates the Metastatic Journey. Dev Cell 49, 332-346, doi:10.1016/j.devcel.2019.03.026 (2019).

13 Schvartz, I., Seger, D. & Shaltiel, S. Vitronectin. Int J Biochem Cell Biol 31, 539-544, doi:10.1016/s1357-2725(99)00005-9 (1999).

14 Bonnans, C., Chou, J. & Werb, Z. Remodelling the extracellular matrix in development and disease. Nat Rev Mol Cell Biol 15, 786-801, doi:10.1038/nrm3904 (2014).

15 Olivares, O. et al. Collagen-derived proline promotes pancreatic ductal adenocarcinoma cell survival under nutrient limited conditions. Nat Commun 8, 16031, doi:10.1038/ncomms16031 (2017).

16 Chen, Y. et al. Type I collagen deletion in alphaSMA(+) myofibroblasts augments immune suppression and accelerates progression of pancreatic cancer. Cancer Cell 39, 548-565 e546, doi:10.1016/j.ccell.2021.02.007 (2021).

17 Deer, E. L. et al. Phenotype and genotype of pancreatic cancer cell lines. Pancreas 39, 425-435, doi:10.1097/MPA.0b013e3181c15963 (2010).

18 Yang, J. et al. Ferroptosis: At the Crossroad of Gemcitabine Resistance and Tumorigenesis in Pancreatic Cancer. Int J Mol Sci 22, doi:10.3390/ijms222010944 (2021).

19 Hung, S. W., Mody, H. R. & Govindarajan, R. Overcoming nucleoside analog chemoresistance of pancreatic cancer: a therapeutic challenge. Cancer Lett 320, 138-149, doi:10.1016/j.canlet.2012.03.007 (2012).

20 Amrutkar, M. & Gladhaug, I. P. Pancreatic Cancer Chemoresistance to Gemcitabine. Cancers (Basel) 9, doi:10.3390/cancers9110157 (2017).

21 Nielsen, M. F., Mortensen, M. B. & Detlefsen, S. Key players in pancreatic cancer-stroma interaction: Cancer-associated fibroblasts, endothelial and inflammatory cells. World J Gastroenterol 22, 2678-2700, doi:10.3748/wjg.v22.i9.2678 (2016).

22 Love, M. I., Huber, W. & Anders, S. Moderated estimation of fold change and dispersion for RNA-seq data with DESeq2. Genome Biol 15, 550, doi:10.1186/s13059-014-0550-8 (2014).

23 Kolde, R. pheatmap: Pretty Heatmaps. R package version 1.0.12. (2019).

24 Chen, E. Y. et al. Enrichr: interactive and collaborative HTML5 gene list enrichment analysis tool. BMC Bioinformatics 14, 128, doi:10.1186/1471-2105-14-128 (2013).

25 Kai, F. et al. ECM dimensionality tunes actin tension to modulate endoplasmic reticulum function and spheroid phenotypes of mammary epithelial cells. EMBO J 41, e109205, doi:10.15252/embj.2021109205 (2022).

26 Kapalczynska, M. et al. 2D and 3D cell cultures - a comparison of different types of cancer cell cultures. Arch Med Sci 14, 910-919, doi:10.5114/aoms.2016.63743 (2018).

27 Yamauchi, M., Barker, T. H., Gibbons, D. L. & Kurie, J. M. The fibrotic tumor stroma. J Clin Invest 128, 16-25, doi:10.1172/JCI93554 (2018).

28 Tian, C. et al. Proteomic analyses of ECM during pancreatic ductal adenocarcinoma progression reveal different contributions by tumor and stromal cells. Proc Natl Acad Sci U S A 116, 19609-19618, doi:10.1073/pnas.1908626116 (2019).

29 Helleman, J. et al. Association of an extracellular matrix gene cluster with breast cancer prognosis and endocrine therapy response. Clin Cancer Res 14, 5555-5564, doi:10.1158/1078-0432.CCR-08-0555 (2008).

30 Hu, D. et al. Stromal fibronectin expression in patients with resected pancreatic ductal adenocarcinoma. World J Surg Oncol 17, 29, doi:10.1186/s12957-019-1574-z (2019).

31 Laklai, H. et al. Genotype tunes pancreatic ductal adenocarcinoma tissue tension to induce matricellular fibrosis and tumor progression. Nat Med 22, 497-505, doi:10.1038/nm.4082 (2016).

32 Armstrong, T. et al. Type I collagen promotes the malignant phenotype of pancreatic ductal adenocarcinoma. Clin Cancer Res 10, 7427-7437, doi:10.1158/1078-0432.CCR-03-0825 (2004).

33 Miyamoto, H. et al. Tumor-stroma interaction of human pancreatic cancer: acquired resistance to anticancer drugs and proliferation regulation is dependent on extracellular matrix proteins. Pancreas 28, 38-44, doi:10.1097/00006676-200401000-00006 (2004).

34 Burris, H. A., 3rd et al. Improvements in survival and clinical benefit with gemcitabine as first-line therapy for patients with advanced pancreas cancer: a randomized trial. J Clin Oncol 15, 2403-2413, doi:10.1200/JCO.1997.15.6.2403 (1997).

35 Bachir, A. I., Horwitz, A. R., Nelson, W. J. & Bianchini, J. M. Actin-Based Adhesion Modules Mediate Cell Interactions with the Extracellular Matrix and Neighboring Cells. Cold Spring Harb Perspect Biol 9, doi:10.1101/cshperspect.a023234 (2017).

36 Schneider, C. A., Rasband, W. S. & Eliceiri, K. W. NIH Image to ImageJ: 25 years of image analysis. Nat Methods 9, 671-675, doi:10.1038/nmeth.2089 (2012).

37 Gjorevski, N. et al. Designer matrices for intestinal stem cell and organoid culture. Nature 539, 560-564, doi:10.1038/nature20168 (2016).

38 S, A. FastQC: A Quality Control Tool for High Throughput Sequence Data [Online]. (2010).

39 Dobin, A. et al. STAR: ultrafast universal RNA-seq aligner. Bioinformatics 29, 15-21, doi:10.1093/bioinformatics/bts635 (2013).

Figure 1

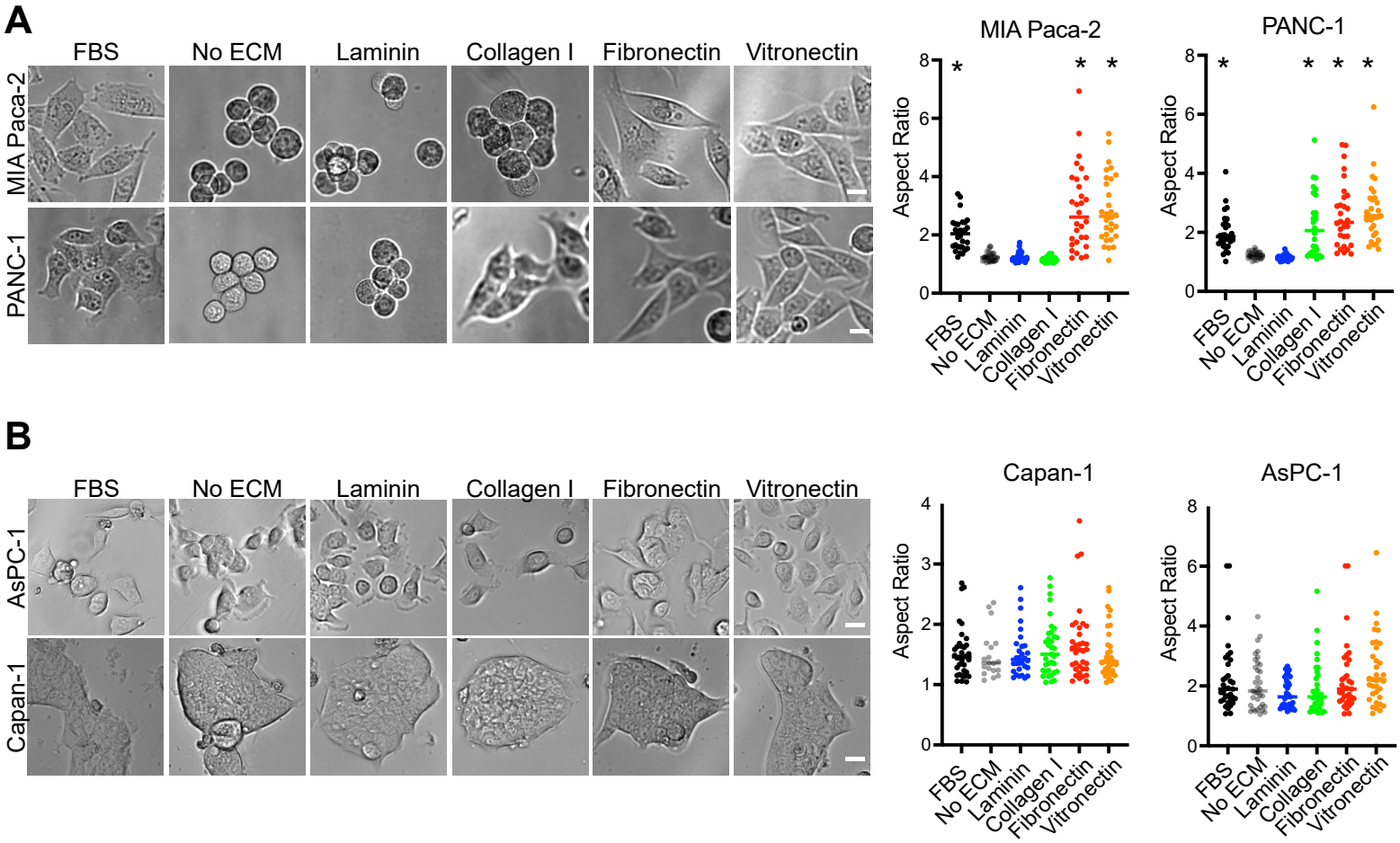
A
FBS
No ECM
Laminin
Collagen I
Fibronectin
Vitronectin
MIA Paca-2
PANC-1
Aspect Ratio
B
AsPC-1
Capan-1
Collagen

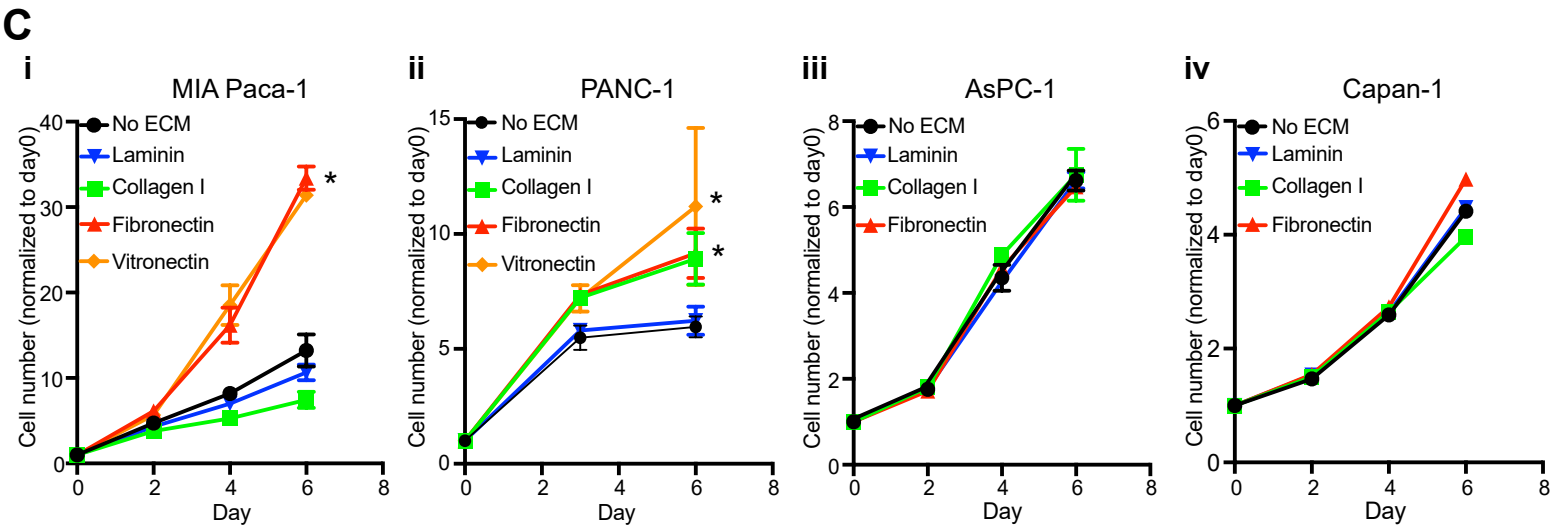
C
i
MIA Paca-1
ii
PANC-1
iii
AsPC-1
iv
Capan-1
No ECM
Laminin
Collagen I
Fibronectin
Vitronectin
Cell number (normalized to day0)
Day

Figure 1. Extracellular matrix proteins have different effects on pancreatic ductal adenocarcinoma (PDAC) cell lines morphology and proliferation.

(A) MIA Paca-2 and PANC-1 cell lines were cultured in media supplemented with either 10% FBS (FBS) or the serum-free supplement, 2% B27. To investigate the effect of ECM proteins, the cells cultured in 2% B27 were seeded on surfaces without (no ECM) or with ECM protein coating: collagen I, laminin, fibronectin, and vitronectin. Representative images show that MIA Paca-2 cells (top) adhere and spread in 10% FBS, and on surfaces coated with fibronectin, and vitronectin. While they have rounded morphology on no ECM, collagen I, and laminin surfaces. The cellular aspect ratio (AR) is significantly higher in MIA Paca-2 cells cultured on fibronectin and vitronectin. For the PANC-1 cells (bottom), they also spread in 10% FBS, and on surfaces coated with collagen I, fibronectin, and vitronectin. While they remain rounded in no ECM and laminin-coated surfaces. The AR for PANC-1 is significantly higher on surfaces coated with collagen I, fibronectin, and vitronectin (N = 3 experiments, n = 30 cells per group, $*p < 0.01$ vs. no ECM, Scale bar: 15 μm)

(B) Capan-1 and AsPC-1 cell lines were cultured with media supplemented with either 10% FBS(FBS) or the serum-free supplement, 2% B27. To study the effect of ECM proteins, the cells cultured in 2% B27 were seeded on surfaces without (no ECM) or with ECM coating: collagen I, fibronectin, and vitronectin. Representative images show that AsPC-1 (top) and Capan-1 (bottom) morphology do not change regardless of the ECM proteins on which they are cultured. The cellular aspect ratio of Capan-1 and AsPC-1 is not different in ECM proteins compared to no ECM.(N = 3 experiments, n = 30 cells per group, $*p < 0.01$ vs no ECM, Scale bar: 15 μm).

(**C**) MIA Paca-2, PANC-1, AsPC1, and Capan-1 cell lines were cultured on surfaces coated with collagen I, fibronectin, laminin, and vitronectin. The number of cells under each condition was quantified on days 2, 4, and 6 using a luminescent cell viability assay. The number of cells on days 2, 4, and 6 was normalized to the number of cells seeded. MIA Paca-2 has a higher proliferation rate on fibronectin and vitronectin substrates compared to collagen I, laminin, or well with no ECM coating (i). PANC-1 cultured on collagen I, fibronectin, and vitronectin show a higher proliferation rate compared to those grown on laminin and no ECM (ii). AsPC1 and Capan-1 cultured on different ECM proteins do not show a difference from those cultured on no ECM plates (iii-iv). (N = 3 experiments, mean±SEM, $*p < 0.01$ vs no ECM).

Figure 2

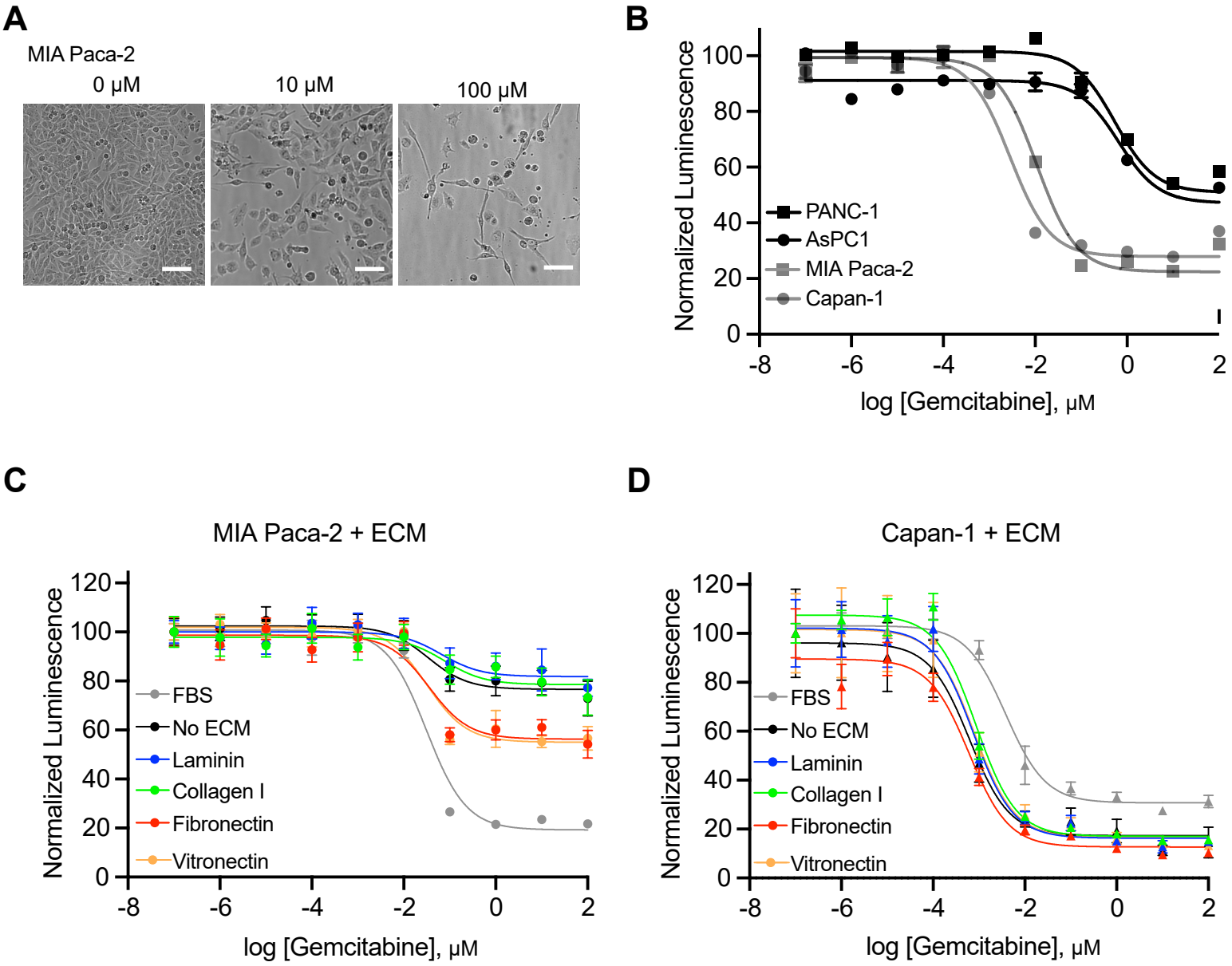
A
MIA Paca-2
0 μM
10 μM
100 μM
B
Normalized Luminescence
PANC-1
AsPC1
MIA Paca-2
Capan-1
log [Gemcitabine], μM
C
MIA Paca-2 + ECM
Normalized Luminescence
FBS
No ECM
Laminin
Collagen I
Fibronectin
Vitronectin
log [Gemcitabine], μM
D
Capan-1 + ECM
Normalized Luminescence
FBS
No ECM
Laminin
Collagen I
Fibronectin
Vitronectin
log [Gemcitabine], μM

Figure 2. Extracellular matrix proteins alter the resistance of MIA Paca-2 to gemcitabine.

(A) Cytotoxic effect of gemcitabine on MIA Paca-2 proliferation was assessed by treating the cell line with different concentrations of the drug. Representative images show that the number of surviving cells decreases with increasing concentrations of gemcitabine (Scale bar: 100 μm).

(B) AsPC-1, Capan-1, MIA Paca-2, and Panc-1 were treated with gemcitabine for 72 hrs and the cell numbers were estimated using luminescence cell viability assay. MIA Paca-2 and Capan-1 are more sensitive to the drug treatment, with IC50 of 10.8 and 2.8 nM, respectively, compared to Panc-1 and AsPC-1 with IC50 of 544.2 and 652.9 nM, respectively.

(C) MIA Paca-2 was cultured on surfaces coated with different ECM proteins and then treated with gemcitabine to study how the ECM proteins affect drug response. The cell viability plot shows that the total number of surviving cells after gemcitabine treatment is the lowest for cells cultured in FBS, followed by the cells cultured on fibronectin and vitronectin, and the cells cultured on collagen I and laminin. (*$p < 0.05$ vs no ECM)

(D) Capan-1 response to gemcitabine in the presence of ECM proteins was estimated by culturing the cells on different ECM proteins and quantifying the number of surviving cells after drug treatment. The viability plot shows that ECM proteins do not significantly alter the decrease in the number of surviving cells following drug treatment.

Figure 3

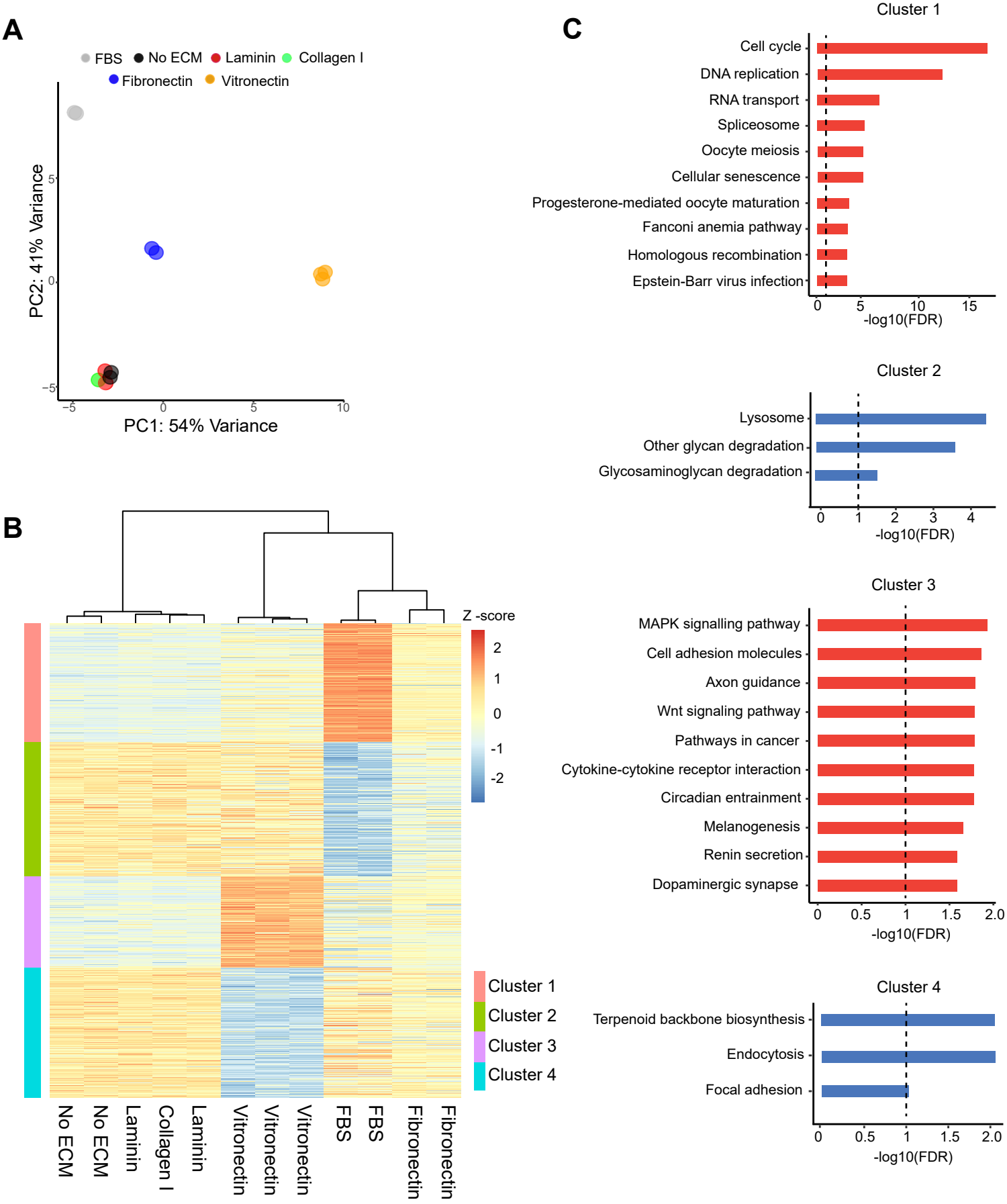
A
FBS
No ECM
Laminin
Collagen I
Fibronectin
Vitronectin
PC2: 41% Variance
PC1: 54% Variance
B
Z -score
2
1
0
-1
-2
Cluster 1
Cluster 2
Cluster 3
Cluster 4
No ECM
No ECM
Laminin
Collagen I
Laminin
Vitronectin
Vitronectin
Vitronectin
FBS
FBS
Fibronectin
Fibronectin
C
Cluster 1
Cell cycle
DNA replication
RNA transport
Spliceosome
Oocyte meiosis
Cellular senescence
Progesterone-mediated oocyte maturation
Fanconi anemia pathway
Homologous recombination
Epstein-Barr virus infection
-log10(FDR)
Cluster 2
Lysosome
Other glycan degradation
Glycosaminoglycan degradation
-log10(FDR)
Cluster 3
MAPK signalling pathway
Cell adhesion molecules
Axon guidance
Wnt signaling pathway
Pathways in cancer
Cytokine-cytokine receptor interaction
Circadian entrainment
Melanogenesis
Renin secretion
Dopaminergic synapse
-log10(FDR)
Cluster 4
Terpenoid backbone biosynthesis
Endocytosis
Focal adhesion
-log10(FDR)

Figure 3. Transcriptomics analysis showing differential gene expression of MIA Paca-2 cells cultured on surfaces coated with ECM proteins.

(A) MIA Paca-2 were cultured on different ECM proteins, and they were subjected to RNA-seq. The gene count across the conditions was normalized using the variance stabilizing transformation from DESeq2. The sample clustering was visualized by plotting the first two components resulting from PCA analysis on the x and y axes respectively. PCA analysis showed that cells on ECM proteins (collagen I, laminin) that result in rounded morphology clustered together with cells grown on no ECM. Interestingly, cells cultured on ECM proteins that result in spread morphology (fibronectin and vitronectin) cluster separately from each other, and the cells cultured in 10% FBS.

(B) Heatmap showing normalized read counts of the differentially regulated genes, which were derived from the comparison between MIA Paca-2 cells cultured on the different ECM proteins against the cells cultured on the surface without ECM coating (no ECM). Clustering analysis of the heatmap reveals that cells cultured on collagen I, laminin, and no ECM protein have a similar expression pattern while those cultured on fibronectin, vitronectin, and FBS show differential gene expression patterns. Cluster 1 comprises genes that are highly upregulated in cells cultured in 10% FBS, while also generally upregulated in cells cultured on vitronectin and fibronectin. Cluster 2 comprises genes that are downregulated in cells cultured in 10% FBS. Clusters 3 and 4 comprise genes that are upregulated and downregulated in cells cultured on a surface coated with vitronectin, respectively. Significant differently expressed genes (adjusted p-value < 0.05, abs($\log_2$FC) > 0.58) in all the ECM proteins were combined and clustered by K-mean (with centers = 4) resulting in the color-coded clusters. Hierarchical clustering was used to cluster the column using Pearson's correlation and Ward.D2.

(C) Bar plot showing the KEGG pathways that are enriched by the regulated genes within the clusters derived from the heatmap in Fig. 3B. The genes within each cluster were subjected to pathway analysis using the Enrichr and the top 10 significant pathways were selected (FDR $<$ 0.1). The Red and blue bars indicate upregulated and downregulated pathways, respectively. The dashed line on the bar plot indicates the FDR cut-off.

Figure 4

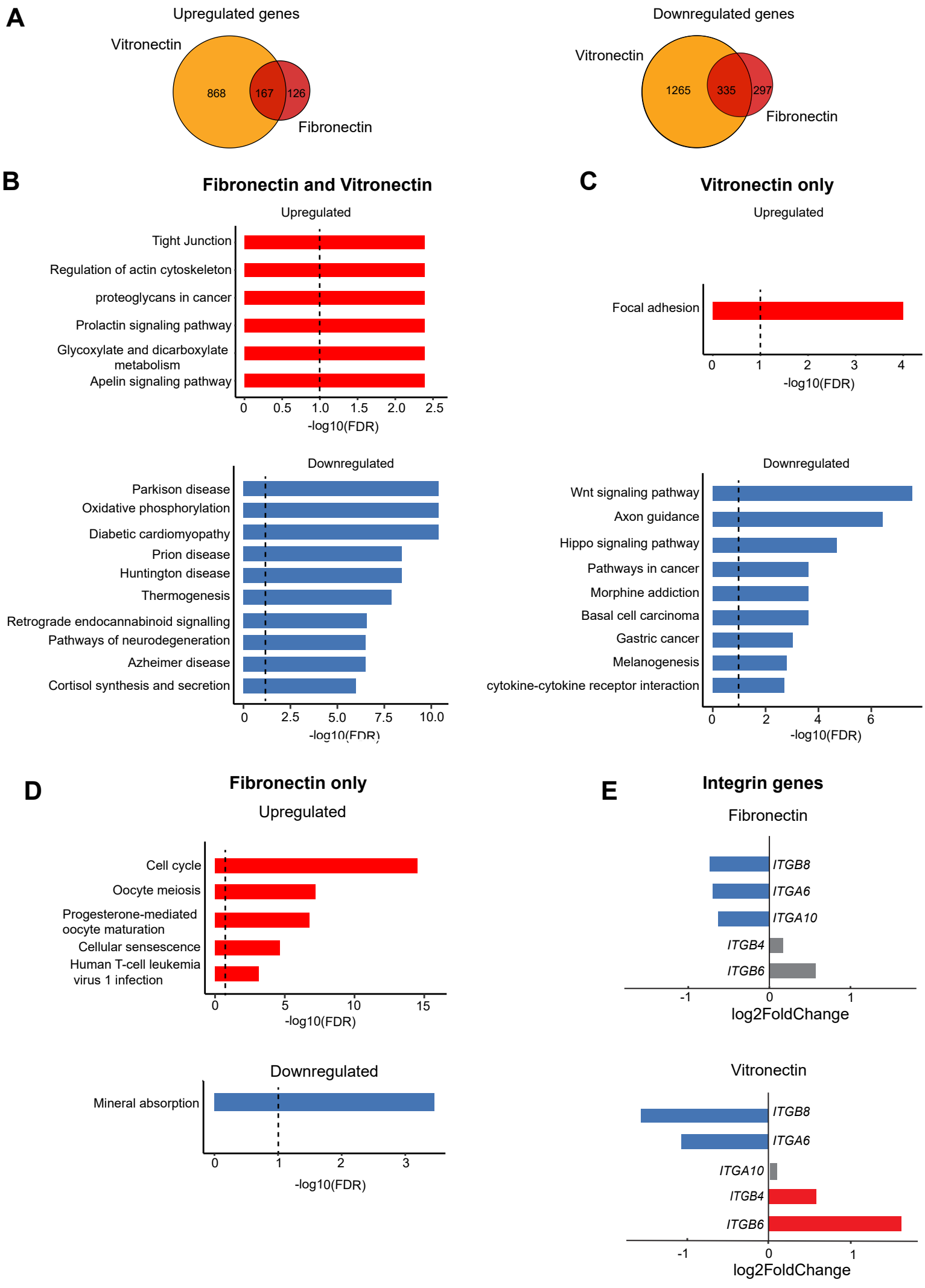
A
Upregulated genes
Vitronectin
868
167
126
Fibronectin
Downregulated genes
Vitronectin
1265
335
297
Fibronectin
B
Fibronectin and Vitronectin
Upregulated
Tight Junction
Regulation of actin cytoskeleton
proteoglycans in cancer
Prolactin signaling pathway
Glycoxylate and dicarboxylate metabolism
Apelin signaling pathway
0
0.5
1.0
1.5
2.0
2.5
-log10(FDR)
Downregulated
Parkison disease
Oxidative phosphorylation
Diabetic cardiomyopathy
Prion disease
Huntington disease
Thermogenesis
Retrograde endocannabinoid signalling
Pathways of neurodegeneration
Azheimer disease
Cortisol synthesis and secretion
0
2.5
5.0
7.5
10.0
-log10(FDR)
C
Vitronectin only
Upregulated
Focal adhesion
0
1
2
3
4
-log10(FDR)
Downregulated
Wnt signaling pathway
Axon guidance
Hippo signaling pathway
Pathways in cancer
Morphine addiction
Basal cell carcinoma
Gastric cancer
Melanogenesis
cytokine-cytokine receptor interaction
0
2
4
6
-log10(FDR)
D
Fibronectin only
Upregulated
Cell cycle
Oocyte meiosis
Progesterone-mediated oocyte maturation
Cellular sensescence
Human T-cell leukemia virus 1 infection
0
5
10
15
-log10(FDR)
Downregulated
Mineral absorption
0
1
2
3
-log10(FDR)
E
Integrin genes
Fibronectin
ITGB8
ITGA6
ITGA10
ITGB4
ITGB6
-1
0
1
log2FoldChange
Vitronectin
ITGB8
ITGA6
ITGA10
ITGB4
ITGB6
-1
0
1
log2FoldChange

Figure 4. MIA Paca-2 cells respond differently to fibronectin and vitronectin.

(A) Venn Diagram showing the number of differentially expressed genes (vs. no ECM) that are regulated in both fibronectin and vitronectin (overlap), and also the ones that are unique to fibronectin or vitronectin. The left panel shows that 167 genes are upregulated in cells cultured on fibronectin and vitronectin while 868 and 126 genes are uniquely upregulated in vitronectin and fibronectin, respectively. The right panel shows that 335 genes are downregulated in cells grown on fibronectin and vitronectin, while 1265 and 297 genes are downregulated uniquely in vitronectin and fibronectin, respectively.

(B) Bar plot showing the KEGG pathways that are enriched by the genes regulated in both fibronectin and vitronectin. The genes in the overlap of the Venn diagrams in Fig. 4A were subjected to pathway analysis using the Enrichr and a maximum of the top 10 significant KEGG pathways were selected (FDR < 0.1). The red and blue bars indicate upregulated and downregulated pathways respectively.

(C) Bar plot showing the KEGG pathways that are enriched by the genes that are uniquely regulated in vitronectin. These genes were subjected to pathway analysis using the Enrichr and a maximum of the top 10 significant KEGG pathways were selected (FDR < 0.1). The red and blue bars indicate upregulated and downregulated pathways respectively

(D) Bar plot showing the KEGG pathways that are enriched by genes that are uniquely regulated in fibronectin. The genes were subjected to pathway analysis using the Enrichr and a maximum of the top 10 significant KEGG pathways were selected (FDR < 0.1). The red and blue bars indicate upregulated and downregulated pathways respectively.

(E) Bar plot showing the fold change of integrins in MIA Paca-2 cell line cultured in fibronectin and vitronectin. Red, blue, and grey bars indicate upregulated, downregulated, and non-significant genes respectively. (control = MIA Paca-2 cells cultured on an uncoated well plate)

Figure S1

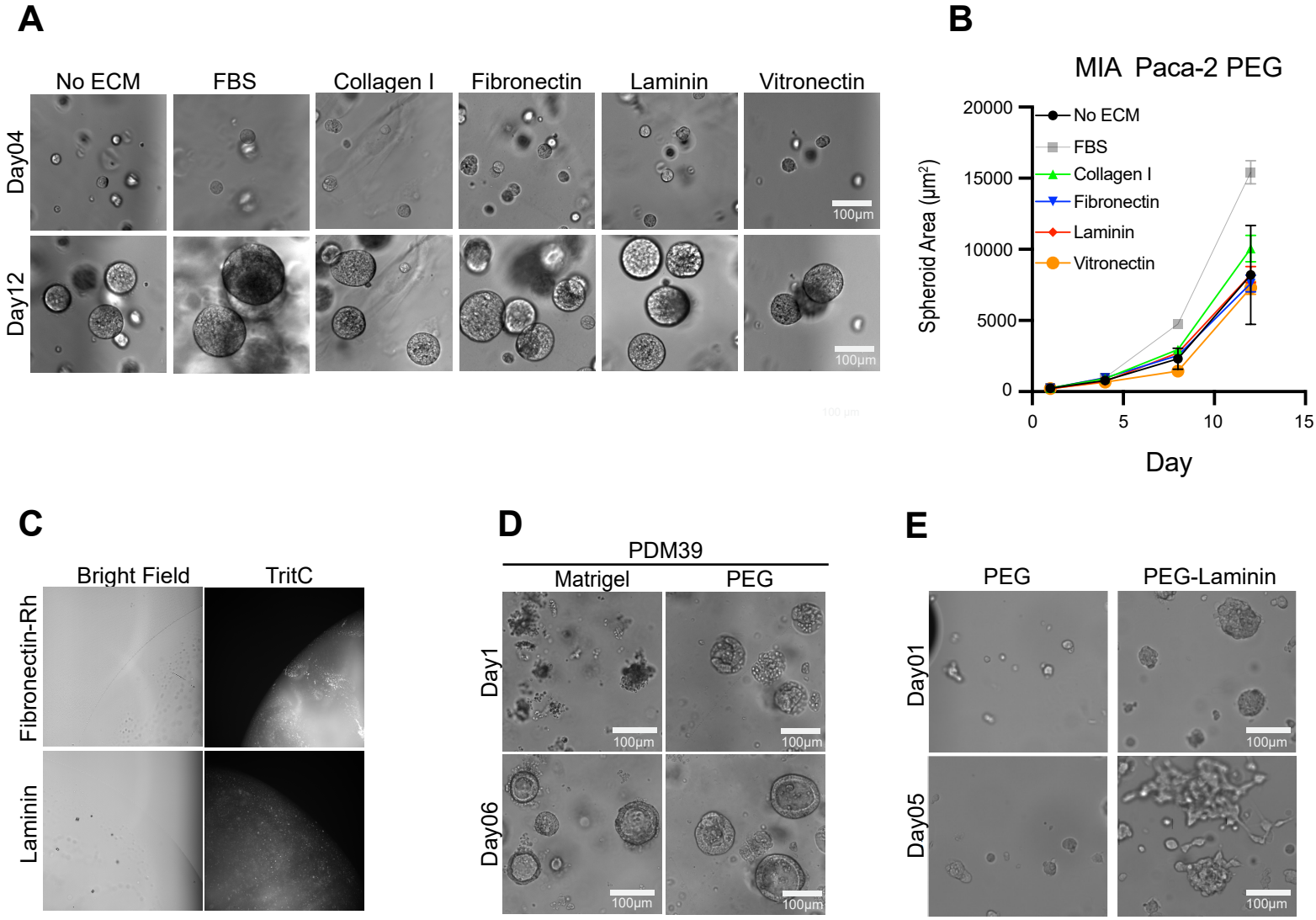
A
No ECM
FBS
Collagen I
Fibronectin
Laminin
Vitronectin
Day04
Day12
100µm
B
MIA Paca-2 PEG
Spheroid Area (µm²)
20000
15000
10000
5000
0
No ECM
FBS
Collagen I
Fibronectin
Laminin
Vitronectin
0
5
10
15
Day
C
Bright Field
TritC
Fibronectin-Rh
Laminin
D
PDM39
Matrigel
PEG
Day1
Day06
100µm
E
PEG
PEG-Laminin
Day01
Day05
100µm

Supplementary S1: MIA Paca-2 cells grow at a similar rate within PEG hydrogel containing various ECM proteins.

(A) Representative images showing the growth of MIA Paca-2 spheroids within PEG gels conjugated with different ECM proteins (scale bar: 100 μm).

(B) MIA Paca-2 cells embedded in PEG gels conjugated with ECM proteins were cultured for 12 days and the growth was quantified by measuring the area of the spheroids. The plot shows that the MIA Paca-2 spheroids grow faster when cultured in 10% FBS, however, the spheroids cultured within the PEG gels with various ECM proteins grow at a similar rate as the spheroids embedded in the PEG gels without any ECM proteins (no ECM) (*$p < 0.05$ vs no ECM).

(C) Immunofluorescence shows the incorporation of ECM proteins into the PEG hydrogel.

(D)PDAC organoid, PDM39 was cultured in Matrigel and PEG for 6 days. Representative images show that the organoid grows both in PEG and Matrigel.

(E) PDM121 was cultured in PEG with no ECM (PEG) and PEG with laminin (PEG-Laminin). Representative images show that PDM121 migrates only in PEG-Laminin.